Supplementary information for manuscript

Burning of Olive Tree Branches: A Major Organic Aerosol Emission Source in the Mediterranean

Evangelia Kostenidou[1], Christos Kaltsonoudis[1,2], Maria Tsiflikiotou[1,2], Evangelos Louvaris[1,2], Lynn M. Russell[4] and Spyros, N. Pandis[1,2,3]

[1]Institute of Chemical Engineering Sciences, ICE-HT, Patras, Greece

[2]Department of Chemical Engineering, University of Patras, Patras, Greece

[3]Department of Chemical Engineering, Carnegie Mellon University, Pittsburgh, USA

[4]Scripps Institute of Oceanography, University of California, San Diego, 92093, USA

1. GC-MS analysis and extraction procedure

Levoglucosan was extracted from the filter sample with 40 mL of ethylacetate containing 3.6 mM triethylamine under sonication for 1 hour. The extract was then filtered through a PTFE 0.2 μm filter (PALL) and condensed by rotary evaporation to a suitable volume (approximately 1 mL, weighted in order to calculate the exact amount). An aliquot (100 μL) of the condensed extract was derivatised with *N*-trimethylsilylimidazole (TMSI) agent (10 μL) for 1 hour at ambient temperature prior to GC-MS analysis.

The GC-MS system consisted of a Shimadzu QP2010 Ultra equipped with an AOC 20i autoinjector. 1 μl of the sample was injected at split mode (1:50). The injector was set at 250 ^{0}C. The temperature program for the column (Mega 5 ms, 0.25 mm I.D., 0.25 μm film thickness, 30 m) was as follows: 1 min at 55 ^{0}C, ramp up to 270 ^{0}C at 20 ^{0}C min^{-1}, 0.25 min at 270 ^{0}C. Helium was used as carrier gas at 1mL min^{-1}. The temperatures for the ion source for the interface between the GC and the MS were set to 170 ^{0}C and 200 ^{0}C respectively. The range of 35-350 atomic mass units was acquired.

Total Ion Count (TIC) was used for the quantification of levoglucosan. The calibration curve was linear in the range between 1-50 μg mL^{-1} (R^2=0.999). The identification of levoglucosan was based on mass spectra and retention time of the standard compound as well as comparison with mass spectra libraries. The recovery was estimated to be 91.8% for teflon and 90.4% for quartz filters, based on spiked filters in the range of 10 μg per filter. The entire Teflon filter was used for each analysis, while for the high volume quartz filters, analysis was done at a punch of 1.5 cm^2, in order to compare with Sunset results (by using punches of the same filter). If the levoglucosan concentration was low (outside the linear range of the calibration curve) a new analysis was performed for the same filter using two or more punches.

2. Comparison of the fresh mass spectra between the 4 source experiments

Table S1. Angle θ between the organic mass spectra of the 4 burning chamber experiments.

Exp Number	**1**	**2**	**3**	**4**
1	0	10.5	5.3	7.2
2	10.5	0	13.2	10.5
3	5.3	13.2	0	7.3
4	7.2	10.5	7.3	0

3. PMF Factors and their correlation with various species

Table S2. Correlations between the 3 PMF factors from HR data and inorganic species and selected *m/z* fragments.

R^2	OOA	HOA	otBB-OA
Ammonium	0.73	0.00	0.04
Sulfate	0.58	0.00	0.00
Organics	0.32	0.29	0.63
Nitrate	0.14	0.08	0.61
Chloride	0.01	0.08	0.53
Potassium	0.16	0.07	0.34
CO_2^+ (m/z 44)	0.87	0.02	0.19
$C_nH^+_{2n-1}$			
C_2H_3 (m/z 27)	0.30	0.14	0.74
C_3H_5 (m/z 41)	0.08	0.41	0.69
C_4H_7 (m/z 55)	0.01	0.79	0.43
C_5H_9 (m/z 69)	0.00	0.92	0.27
$C_nH^+_{2n+1}$			
C_2H_5 (m/z 29)	0.09	0.40	0.70
C_3H_7 (m/z 43)	0.01	0.88	0.33
C_4H_9 (m/z 57)	0.00	0.97	0.18
$C_nH_{2n-3}O^+$			
C_2HO (m/z 41)	0.19	0.02	0.01
C_3H_3O (m/z 55)	0.27	0.10	0.73
C_4H_5O (m/z 69)	0.43	0.02	0.66
$C_nH_{2n-1}O^+$			
CHO (m/z 29)	0.00	0.00	0.03
C_2H_3O (m/z 43)	0.58	0.05	0.52
C_3H_5O (m/z 57)	0.23	0.07	0.83
Levoglucosan			
$C_2H_4O_2$ (m/z 60)	0.14	0.07	0.87
$C_3H_5O_2$ (m/z 73)	0.14	0.08	0.87
$C_nH^+_{n-2}$			
C_3H (m/z 37)	0.43	0.07	0.65
C_4H_2 (m/z 50)	0.38	0.08	0.70
C_5H_3 (m/z 63)	0.28	0.09	0.78
C_6H_4 (m/z 76)	0.33	0.09	0.70
C_7H_5 (m/z 89)	0.23	0.08	0.81
C_8H_6 (m/z 102)	0.16	0.08	0.79
C_9H_7 (m/z 115)	0.12	0.17	0.88

4. FTIR filter composition for experiment 2

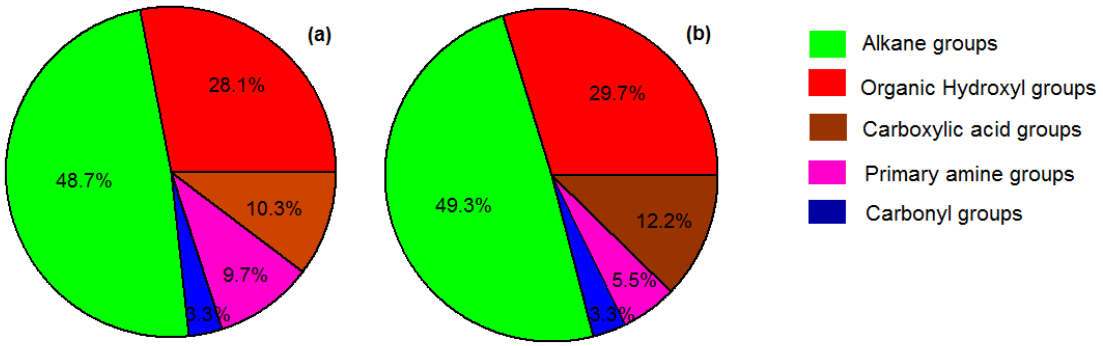

Figure S1. otBB-OA organic functional group composition from FTIR analysis for experiment 2 (a) for the sample taken directly from the olive tree branches fire and (b) from the chamber the first hour of the experiment. One difference is the carboxylic acid contribution, where the more fresh particles contain less carboxylic acids, 10.3%, than the 1 hour aged particles 12.2%.

5. Comparison of mass spectra during experiment 2

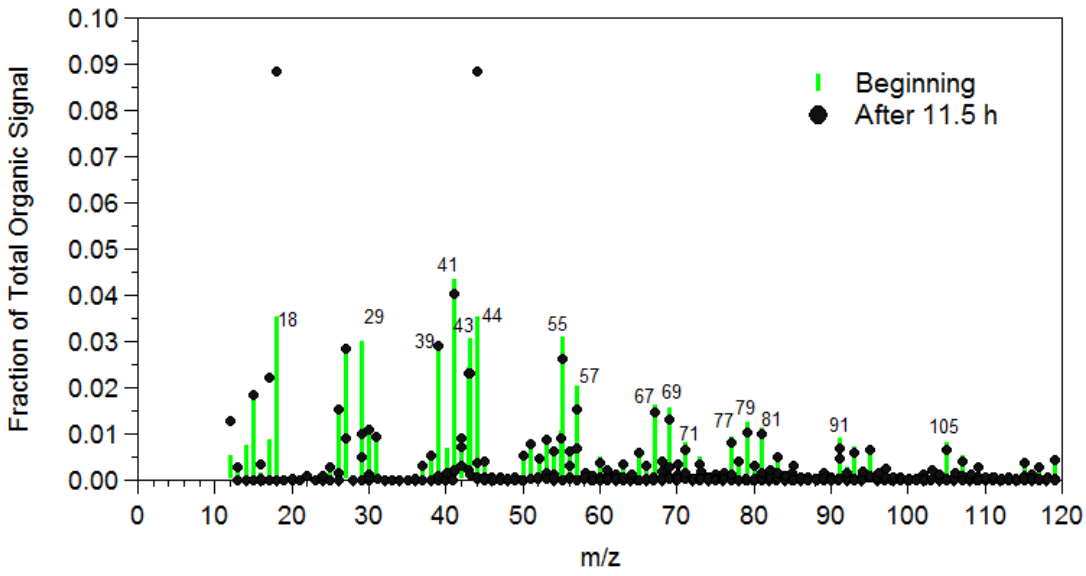

Figure S2. The HR mass spectra at t=0 and t=11.5 h for experiment 2. The f_{44} has increased while the hydrocarbon parts of the $f_{m/z}$*'s*: 29, 39, 41, 43, 55, 57, 67, 69, 71 etc. have decreased.

6. PMF analysis

The selection of the solution was based on the structure of the deconvoluted mass spectra and correlation by comparison between the factor time series and various tracers. The f_{peak} was chosen so the otBB-OA factor is closer to the average otBB-OA mass spectrum obtained from the chamber experiments. The angle θ between the average otBB-OA chamber mass spectrum and the otBB-OA spectrum for f_{peak} in the range -2.0 to 2.0 was calculated (Figure S3) and the f_{peak}=-0.2 was selected as the angle θ was the minimum (10.55 degrees). The angle was less than 17 degrees in all cases so the spectra resembled each other for all f_{peak} choices.

We investigated the 4-factor solution as well. Figures S4 and S5 illustrate the model residuals for 1 to 6 factor solution. Moving from 1 to 2 and from 2 to 3 factors the reduction in the residuals is significant. For the 4-factor solution the residuals are lower only during 16 February 2012 (Figure S5). This day was Fat Thursday in Greece characterized by wide-spread barbequing in Patras, so one would expect additional OA sources. The angle θ between the otBB-OA 4 solution factor and the average otBB-OA mass spectrum from the chamber was calculated (Figure S6) and the best correlation (θ <10 degrees) found between f_{peak} -2 and -0.6. However, in this range the mass spectra of the OOA and the fourth factor are becoming identical (Figure S7). This implies that the 4 factor solution splits the OOA mass spectra into 2 almost identical factors. For f_{peak} -0.4 and 2, the fourth factor has a resemblance with other COA mass spectra e.g from SIRTA and LHVP, during the winter 2010 MEGAPOLI campaign in Paris, (Crippa et al., submitted) as the angle θ is 27 degrees (Figure S8). However, the correlation between the otBB-OA PMF and the average otBB-OA chamber spectrum is becoming worse (Figure S6) and the time series of the otBB-OA and the fourth factor correlate each other as the f_{peak} increases (Figure S9). This means that in the range -0.4 and 2 the PMF tries to create a COA factor but "destroys" in the process the otBB-OA factor.

Performing the PMF analysis excluding the Fat Thursday the 3 factor solution does not practically change compared to the initial selected solution that included the Fat Thursday inputs. The 4 factor solution splits the OOA spectrum into 2 identical spectra for f_{peak} -2 to 2. Doing the PMF analysis for the last 3 days, including the Fat Thursday, the 3 factor solution results in 3 mass spectra: OOA, otBB-OA and a mixture of HOA and COA. Moving to 4 factors we have 2 cases: (a) For f_{peak} in the range -2 to 0.6, the OOA and otBB-OA mass spectra are very close to the OOA and otBB-OA from the 3

factor solution excluding the Fat Thursday (R^2=0.99 and 0.98 correspondingly). However, the HOA mass spectrum has changed (R^2=0.6 in comparison with the HOA excluding the Fat Thursday) and the COA does not correlate well with the literature COA spectra (maximum R^2=0.4). Moreover the COA and HOA mass spectra are quite similar to each other (R^2=0.82). (b) For f_{peaks} between 0.8 and 2 the COA and HOA mass spectra are becoming more independent (R^2=0.63-0.53), but the otBB-OA mass spectrum differs from the chamber otBB-OA mass spectrum (R^2=0.78-0.73) and the COA time series highly correlates the HOA time series (R^2=0.91). This indicates that the extraction of a COA factor is leading to artifacts given the small amount of cooking emissions in our data set. So, we discuss the characteristics of the 3 factor solution from all the 20 days, but we will not apply this solution to the Fat Thursday.

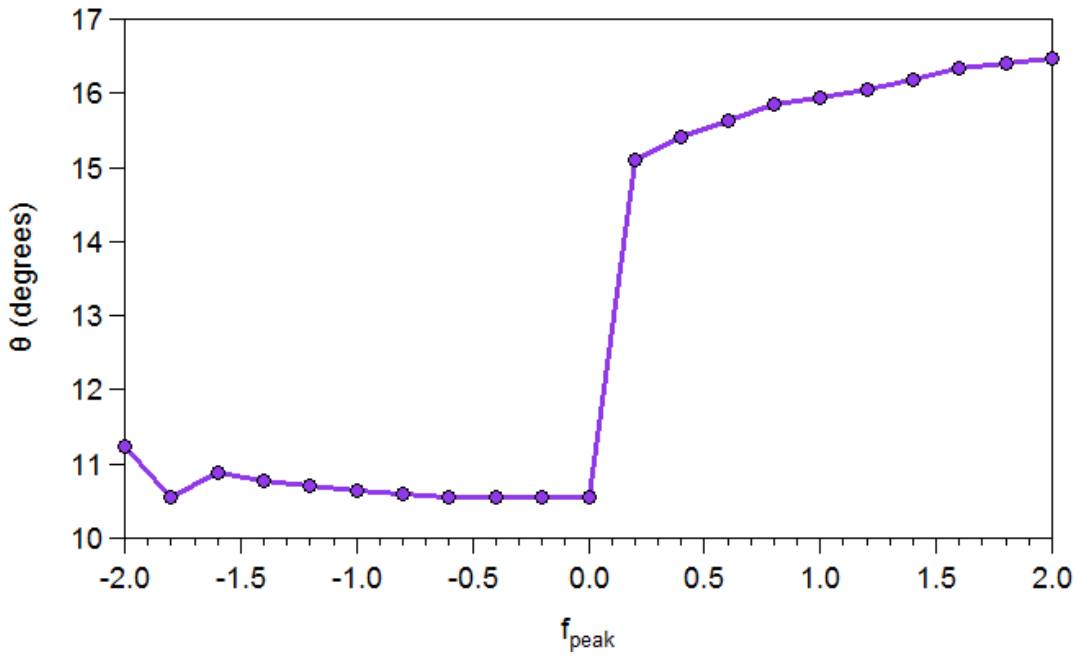

Figure S3. Criteria for the selection of the f_{peak}: We choose the f_{peak} for which the angle θ between the average otBB-OA chamber mass spectrum and the otBB-OA factor profile is minimum (when f_{peak} =-0.2, then θ=10.55 degrees).

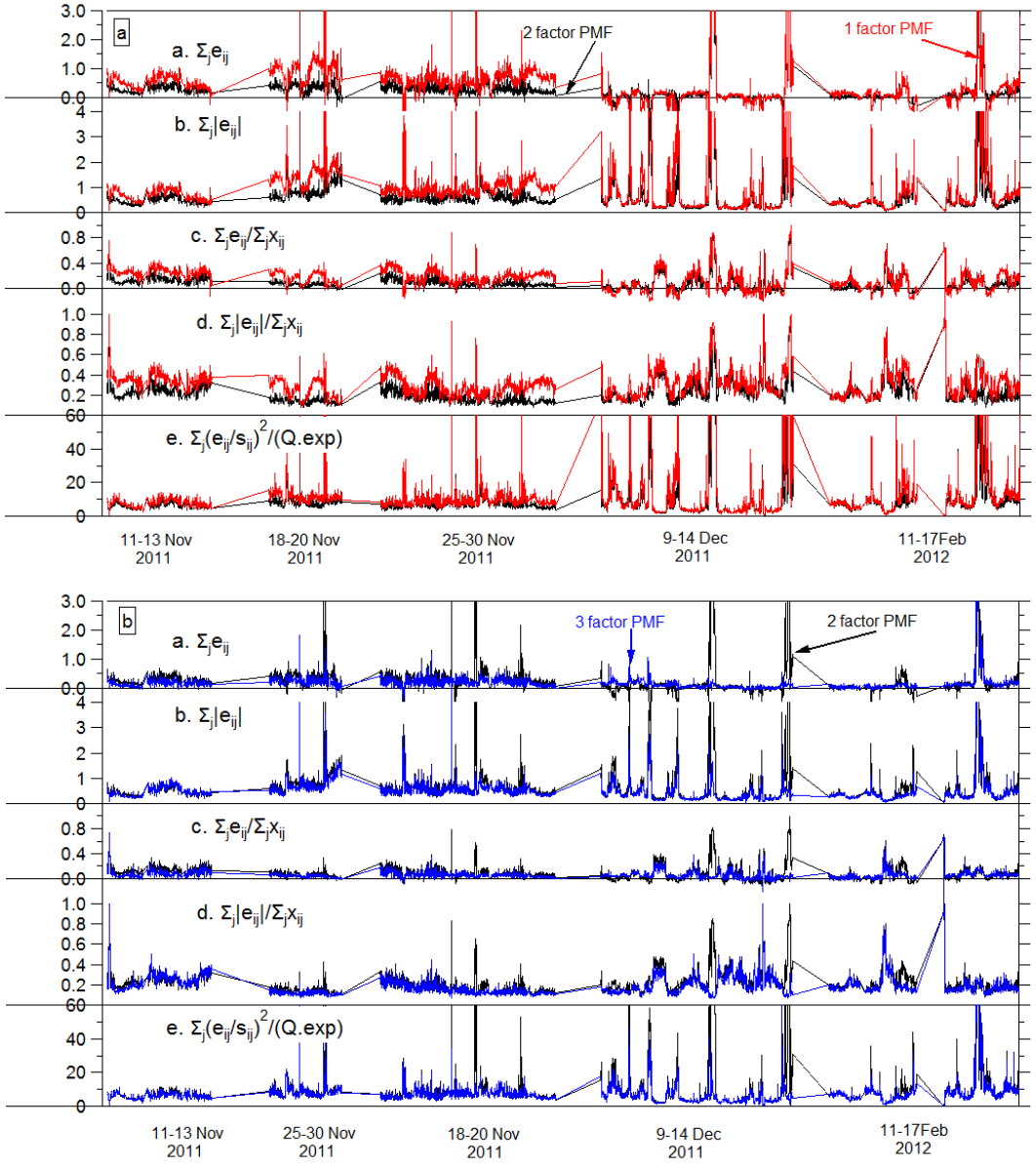

Figure S4. Comparison between model residuals **E= X-GF** (a) for 1-factor (red lines) to 2-factors (black lines) PMF solution and (b) for 2-factors (black lines) to 3-factors (blue lines) PMF solution. The model residuals were calculated in five different ways: (1) sum of residuals, (2) sum of the absolute value of residuals, (3) sum of residuals relative to total organics, (4) sum of absolute value of residuals relative to total organics, and (5) sum of squared, uncertainty-weighted (scaled) residuals, Q(t)=E(t)/S(t), relative to expected values, Qexp(t). The model residuals were estimated using the PMF evaluation tool, PET, by Ulbrich et al. (2009). The structure in the residuals was decreased significantly in the p =2 solution compared to the p =1 solution. Comparing the 2 and 3 factor solutions the residuals decreased significantly from p=2 to p=3 solution.

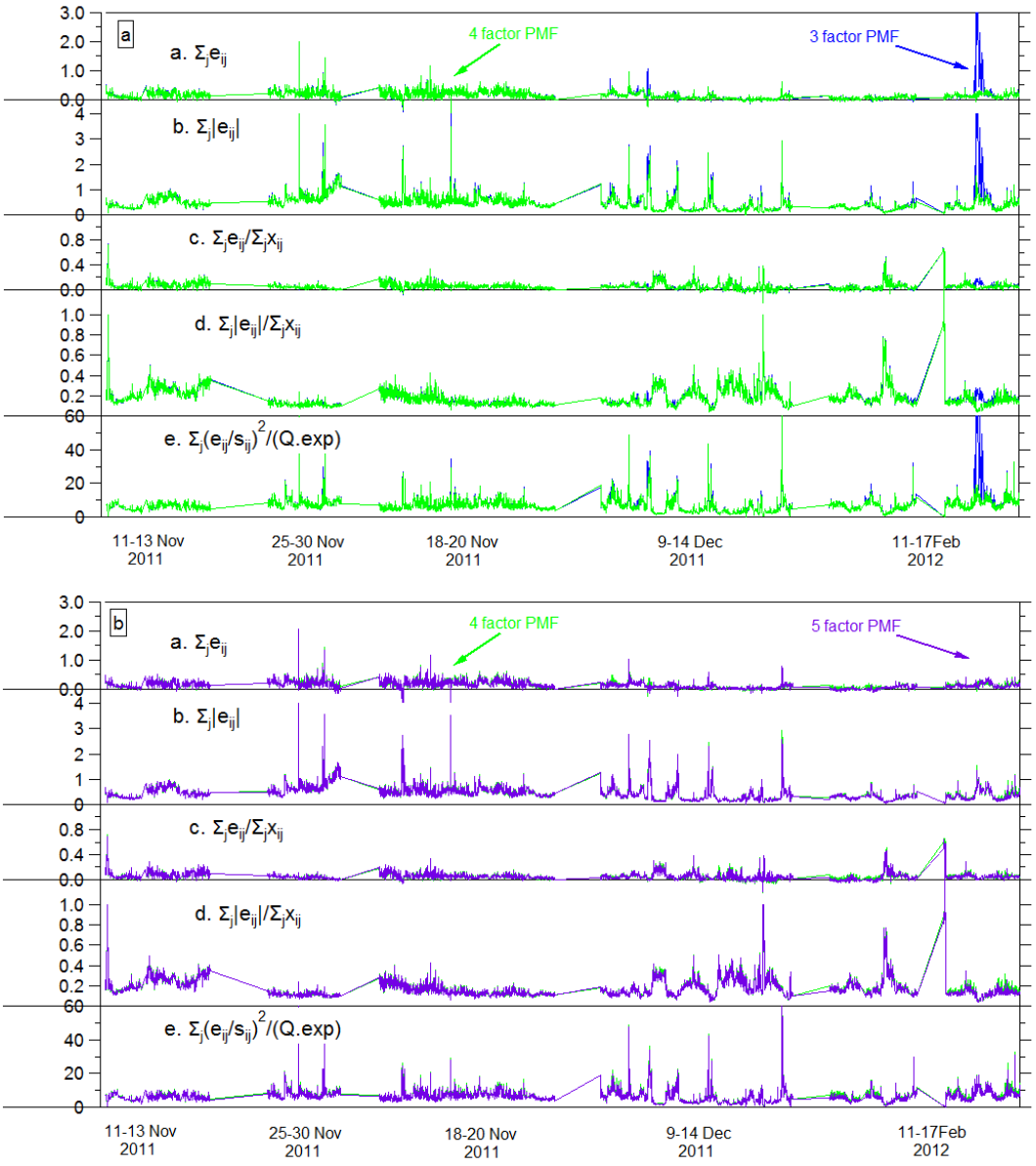

Figure S5. Comparison between model residuals **E= X-GF** (a) for 3-factor (blue lines) to 4-factors (green lines) PMF solution and (b) for 4-factors (green lines) to 5-factors (purple lines) PMF solution. The model residuals were calculated in five different ways: (1) sum of residuals, (2) sum of the absolute value of residuals, (3) sum of residuals relative to total organics, (4) sum of absolute value of residuals relative to total organics, and (5) sum of squared, uncertainty-weighted (scaled) residuals, Q(t)=E(t)/S(t), relative to expected values, Qexp(t). The model residuals were estimated using the PMF evaluation tool, PET, by Ulbrich et al. (2009). The structure in the residuals was decreased significantly in the p =4 solution compared to the p =2 solution only during Fat Thursday 16 February 2012. Comparing the 4 and 5 factor solutions the residuals practically did not change.

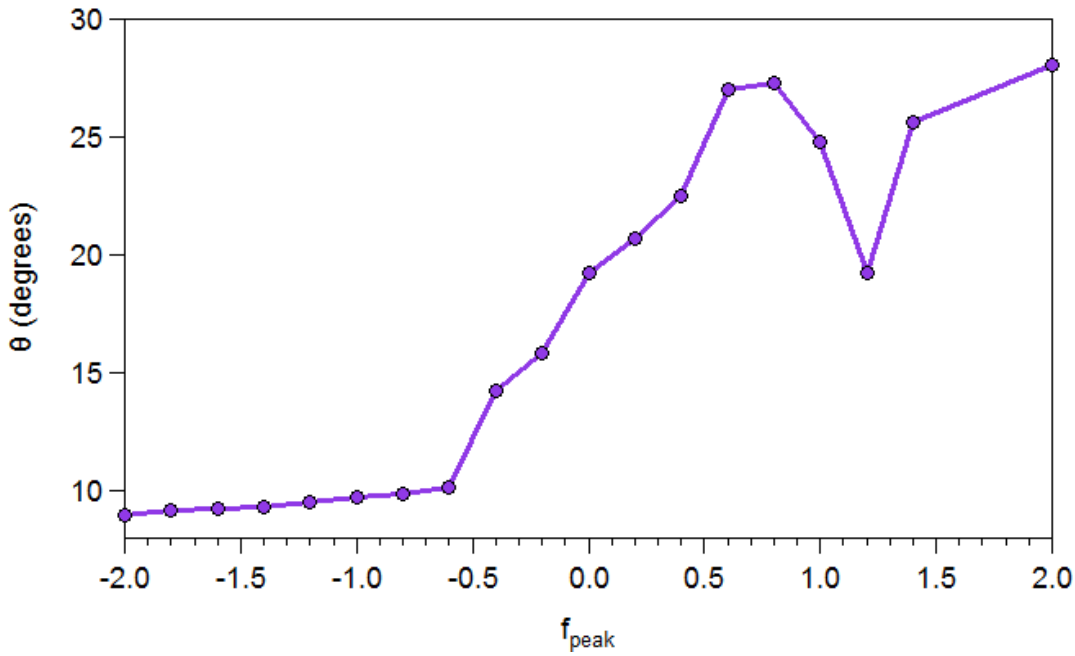

Figure S6. Angle θ between the average otBB-OA chamber mass spectrum and the otBB-OA profile factor from the 4 PMF solution. The lower angle and so the greater resemblance, is in the range f_{peak} -2 to -0.6, but after f_{peak}=-0.4 the two mass spectra deviate each other.

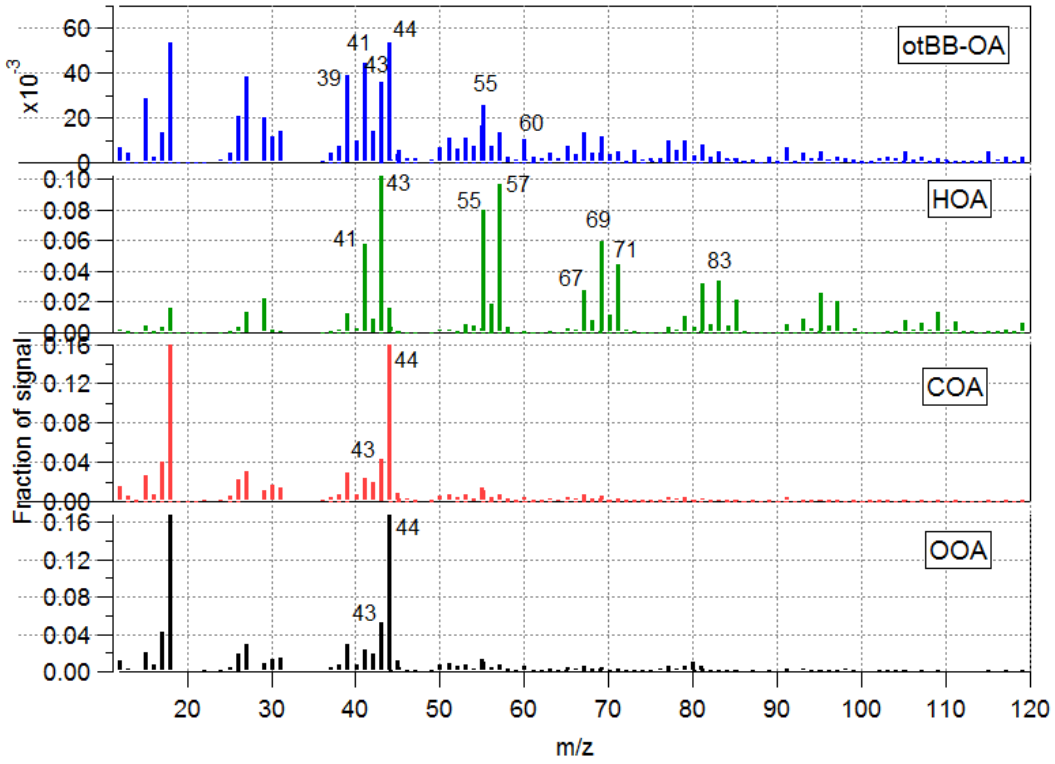

Figure S7. The 4 factor PMF solution for f_{peak}=-1.0. The mass spectrum of the fourth factor is identical to the OOA spectrum (θ=4.7 degrees). This behavior is observed in the f_{peak} range -2 to -0.6.

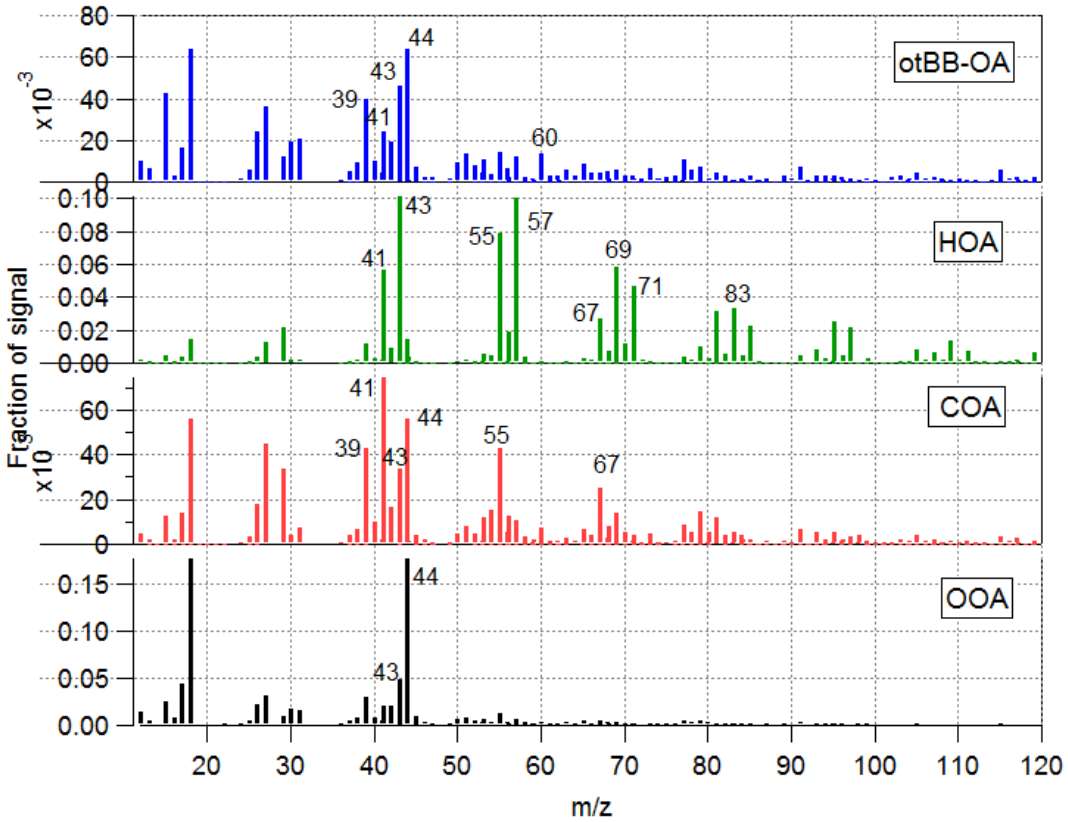

Figure S8. The 4 factor PMF solution for f_{peak}=1.0. The mass spectrum of the fourth factor resembles the COA mass spectra in the literature (θ=27 degrees between the fourth mass spectrum and the COA mass spectra obtained by Crippa et al. (2012)). However the otBB-OA mass spectrum factor deviates from the otBB-OA measured in the chamber (θ=25 degrees). This behavior is typical in the f_{peak} range -0.4 to 2.

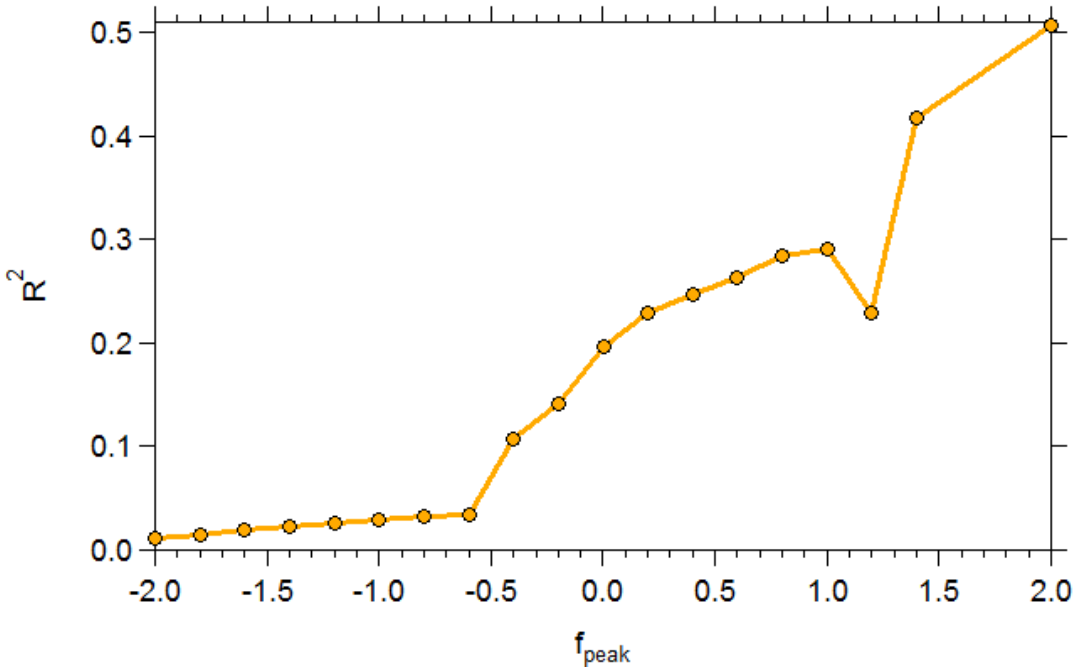

Figure S9. Correlation coefficient R^2 between the time series of the otBB-OA and the fourth factor. For f_{peak} -2 to -0.6 the time series are practically independent, but after -0.6 there is an increasing correlation between them, which suggests a problematic solution.

7. Pump losses calculation

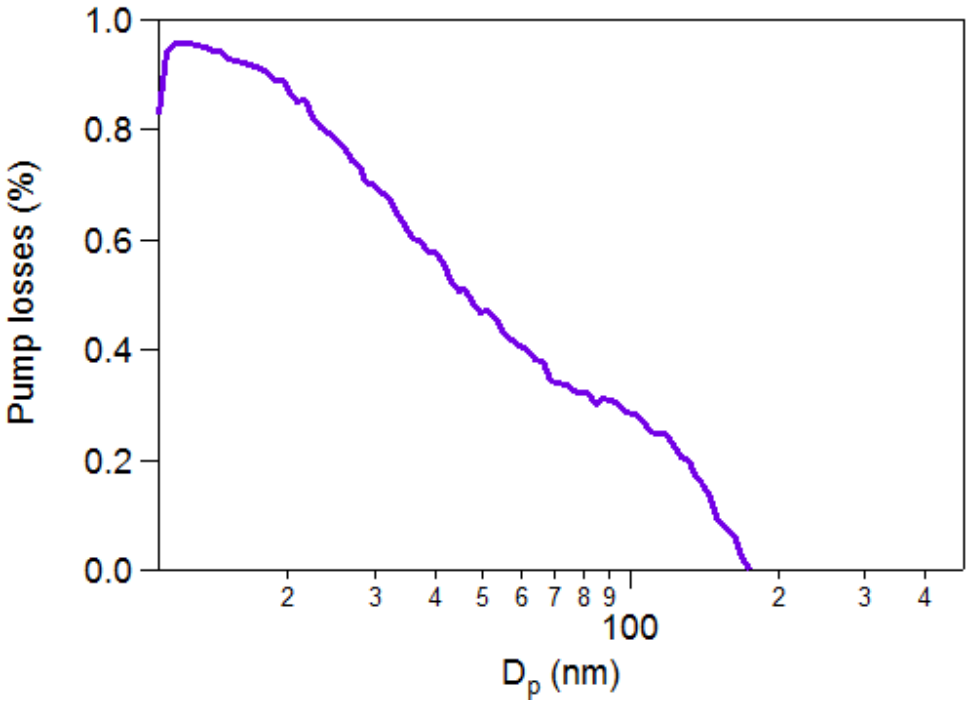

Figure S10. The percent pump loss versus the mobility diameter in nm, measured by 2 SMPS systems.

8. Coagulation of otBB-OA using the model TOMAS

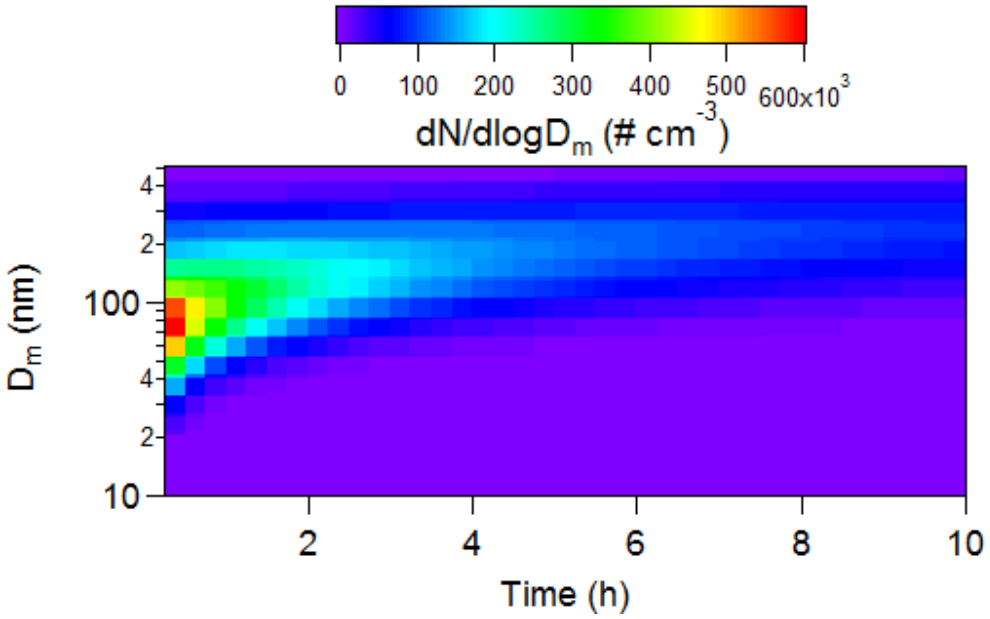

Figure S11. Evolution of ambient otBB-OA size distribution for 500,000 particles cm^{-3}, if there was no dilution, using the model TOMAS (Adams and Seinfeld, 2002). Within 1-2 hours the mode diameter becomes ~115 nm.

References

Adams, P. J., and Seinfeld, J. H.: Predicting global aerosol size distributions in general circulation models, J. Geophys. Res., 107, 4370, 2002.

Crippa, M., DeCarlo, P. F., Slowik, J. G., Mohr, C., Heringa, M. F., Chirico, R., Poulain, L., Freutel, F., Sciare, J., Cozic, J., Di Marco, C. F., Elsasser, M., Jose, N., Marchand, N., Abidi, E., Wiedensohler, A., Drewnick, F., Schneider, J., Borrmann, S., Nemitz, E., Zimmermann, R., Jaffrezo, J.-L., Prevot, A. S. H., and Baltensperger, U.: Wintertime aerosol chemical composition and source apportionment of the organic fraction in the metropolitan area of Paris, Atmos. Chem. Phys. Discuss., 12, 22535–22586, 2012.

Ulbrich, I. M., Canagaratna, M. R., Zhang, Q., Worsnop, D. R., and Jimenez, J. L.: Interpretation of organic components from Positive Matrix Factorization of aerosol mass spectrometric data, Atmos. Chem. Phys., 9, 2891–2918, 2009.